Géodynamo : Observations et Modèles

GdR dynamo, juin 2003

Emmanuel Dormy

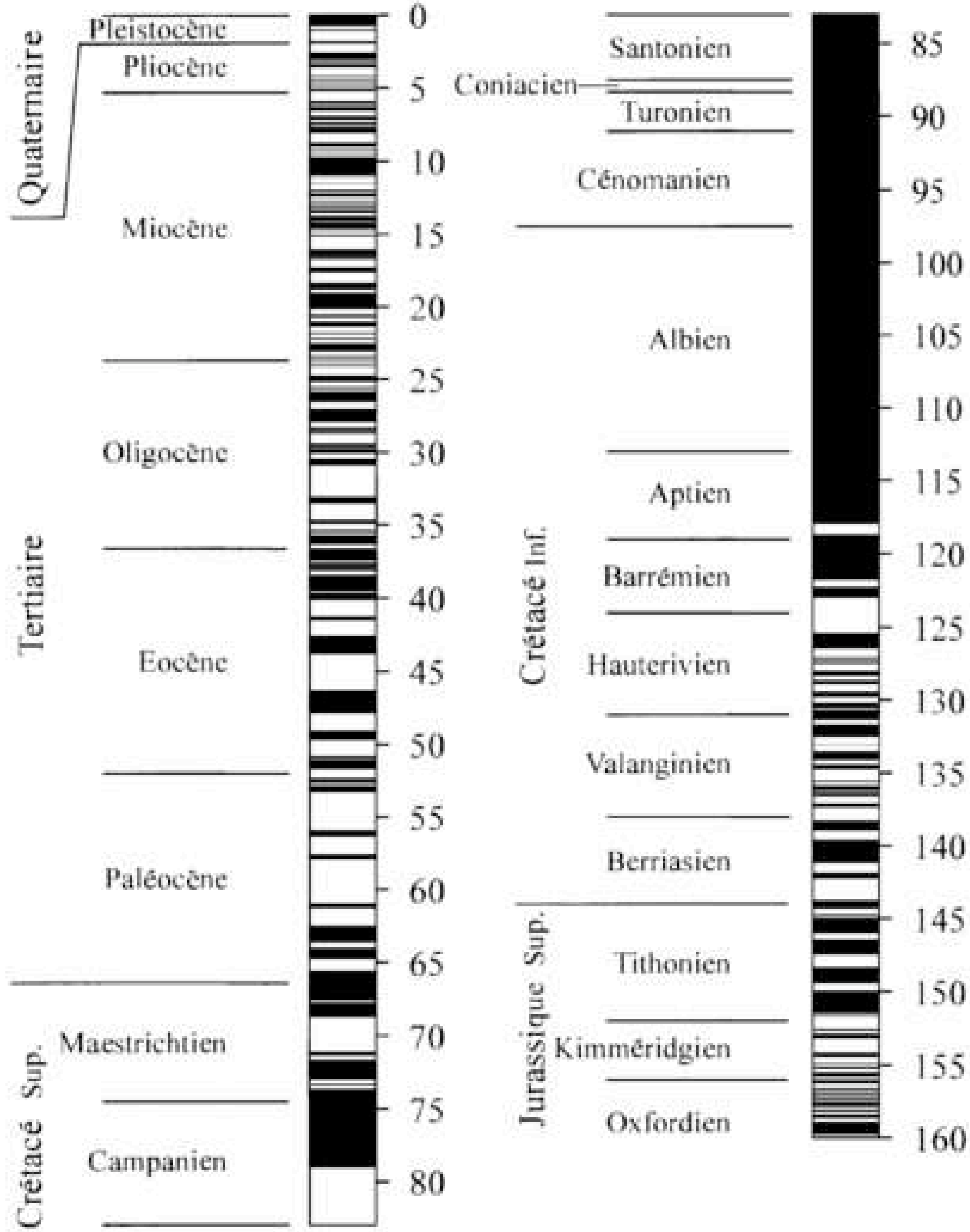
Quaternaire
Pleistocène
Pliocène
Miocène
Tertiaire
Oligocène
Eocène
Paléocène
Crétacé Sup.
Maestrichtien
Campanien
0
5
10
15
20
25
30
35
40
45
50
55
60
65
70
75
80
Santonien
Coniacien
Turonien
Cénomanien
Albien
Aptien
Crétacé Inf.
Barrémien
Hauterivien
Valanginien
Berriasien
Jurassique Sup.
Tithonien
Kimméridgien
Oxfordien
85
90
95
100
105
110
115
120
125
130
135
140
145
150
155
160

Sawtooth, SINT800

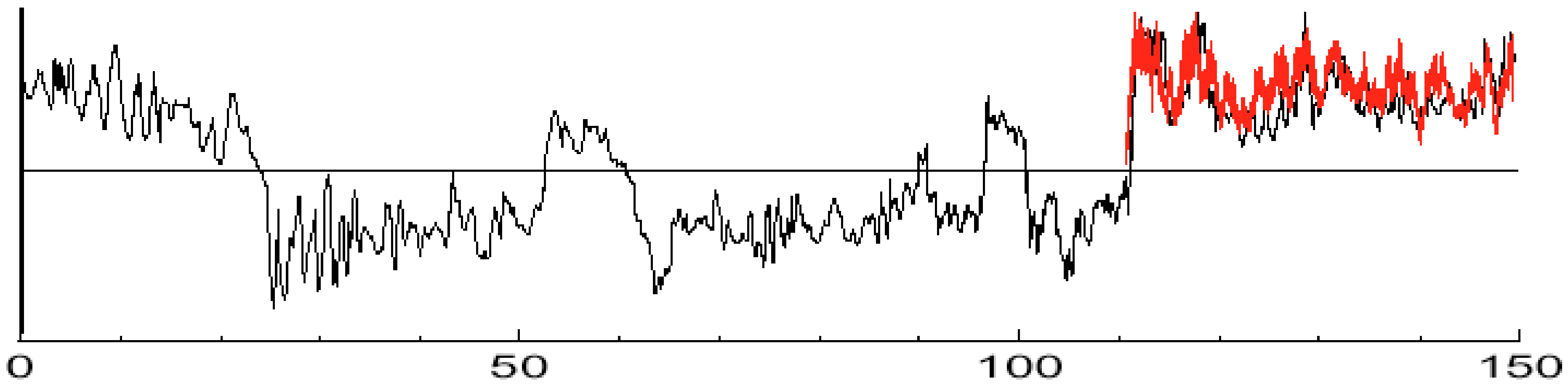

1590

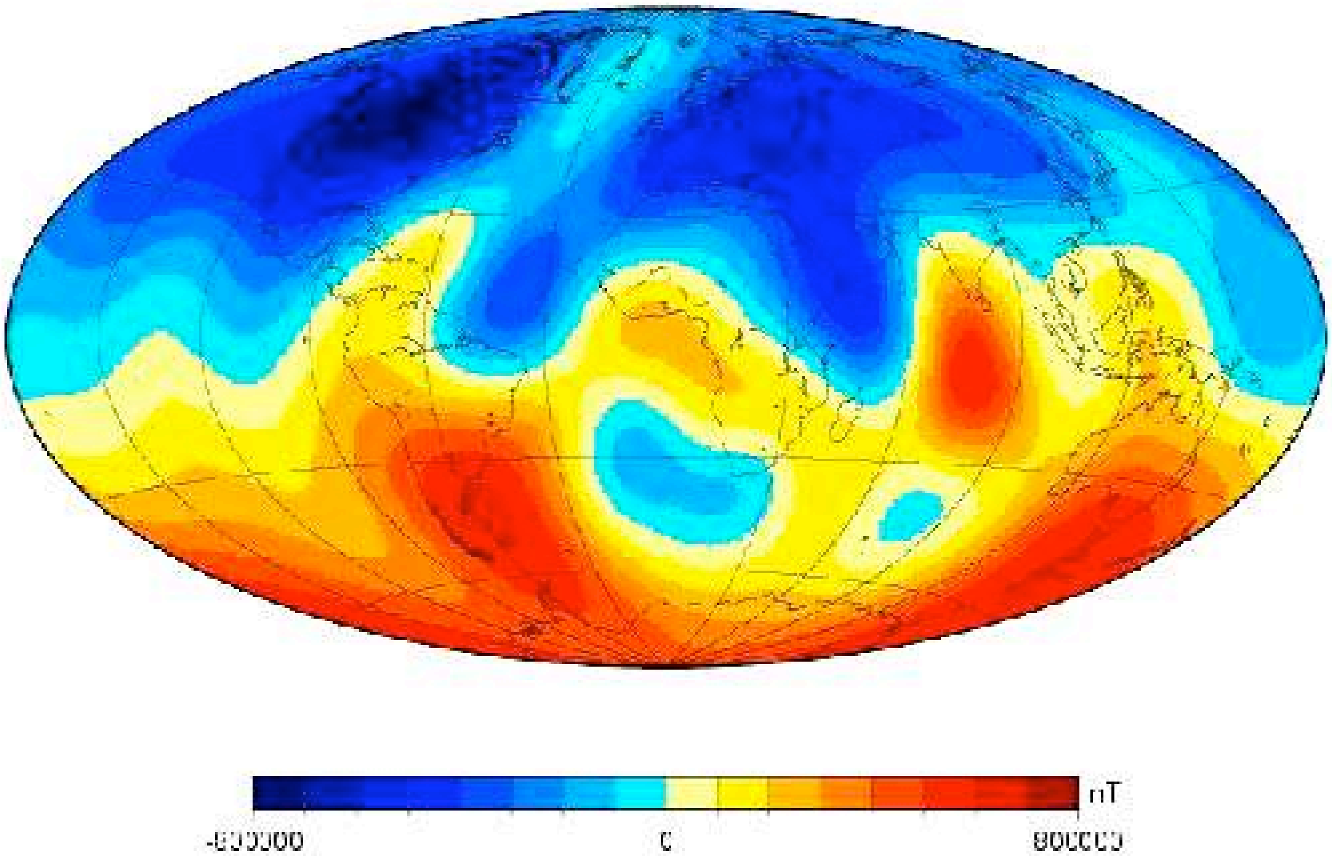

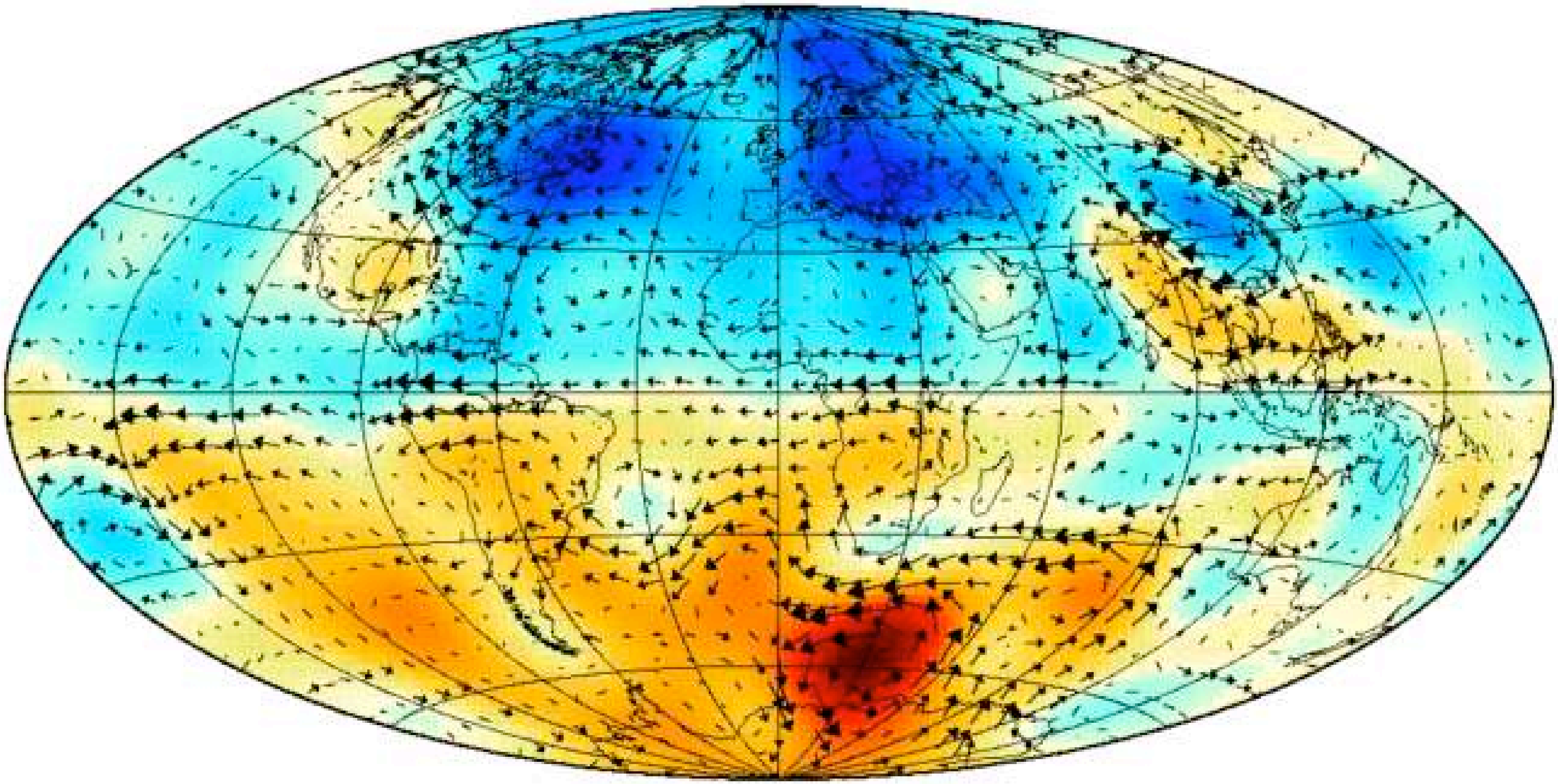

Eymin-Hulot

Time scale	F	D, I	Field characteristic	Multiple Sites	Volcanics & Sediments	Different authors	Controversy	Status
0.1 –1 kyr	x	x	Geomagnetic impulses	y	n.a.	y		A
		x	Geomagnetic impulses during reversals	n	y?	n	y	C
	x	x	Pacific dipole window	y	n.a.	y	y	B
	x	x	Global and systematic westward drift	n	n.a.		y	C
			Columns and patches	y	n.a.	y		A
			Dipole dominates	y	n.a.	y		A
1 – 10 kyr		x	Global and systematic westward drift	n	n.a.	y	y	C
			Excursions and reversals have similar durations shorter than 5 kyr	y	y	y		A
	x	x	Excursions associated with intensity lows	y	y	y		A
	x	x	Reversals dominated by non-dipole components	y	y	y		A
	x	x	Asymmetrical decay and recovery Immediately before and after reversal	y	y	y		B
		x	Preferred longitudes of transitional VGPs	y	n	y	y	B
		x	Long-lived transitional states	y	n	y	y	B

Time scale	F	D, I	Field characteristic	Multiple Sites	Volcanics & Sediments	Different authors	Controversy	Status
10 – 100 kyr	x	x	20 to 60 kyr long oscillations of dipole moment	y	y	y		A
	x	x	Periodic variations of dipole moment	n	n.a.	n	y	C
	x	x	Dipole dominates	y	y	y		A
0.1 - 5Myr	x		Long-term decrease (saw-tooth) during stable polarity	y	y	y	y	B
	x		Average dipole moment between 4 and 6 x 10^{22} $A.m^2$	y	y	y		A
		x	Columns and patches	y	y	y	y	B
	x	x	Dipole dominates	y	y	y		A
		x	$1000 < g_2^0 < 2000$ nT	y	y	y		A
		x	$g_n^m\ h_n^m < 1000$nT	y	y	y		A
>5 Myr		x	Reversal frequency < 6 /Myr	y	y	y		A
		x	Superchrons	y	y	y		A
		x	Mezosoïc dipole low	y		y	y	B

$$
\begin{cases}
Ro\left(\dfrac{\partial \mathbf{u}}{\partial t} + (\mathbf{u}\cdot\boldsymbol{\nabla})\,\mathbf{u}\right) + \mathbf{e}_z \wedge \mathbf{u} = -\boldsymbol{\nabla}\pi - q\,Ra\,E\,T\,\mathbf{g} + E\,\Delta\mathbf{u} \\
\qquad\qquad\qquad\qquad\qquad\qquad + (\boldsymbol{\nabla}\wedge\mathbf{B})\wedge\mathbf{B} \\
\boldsymbol{\nabla}\cdot\mathbf{u} = 0 \\
\dfrac{\partial T}{\partial t} + \mathbf{u}\cdot\boldsymbol{\nabla}T = q\Delta T \\
\dfrac{\partial \mathbf{B}}{\partial t} = \boldsymbol{\nabla}\wedge(\mathbf{u}\wedge\mathbf{B}) + \Delta\mathbf{B}
\end{cases}
$$

$$
Ro = \frac{\eta}{2\Omega\mathcal{L}^2} \qquad E = \frac{\nu}{2\Omega\mathcal{L}^2} \qquad q = \frac{\kappa}{\eta}
$$

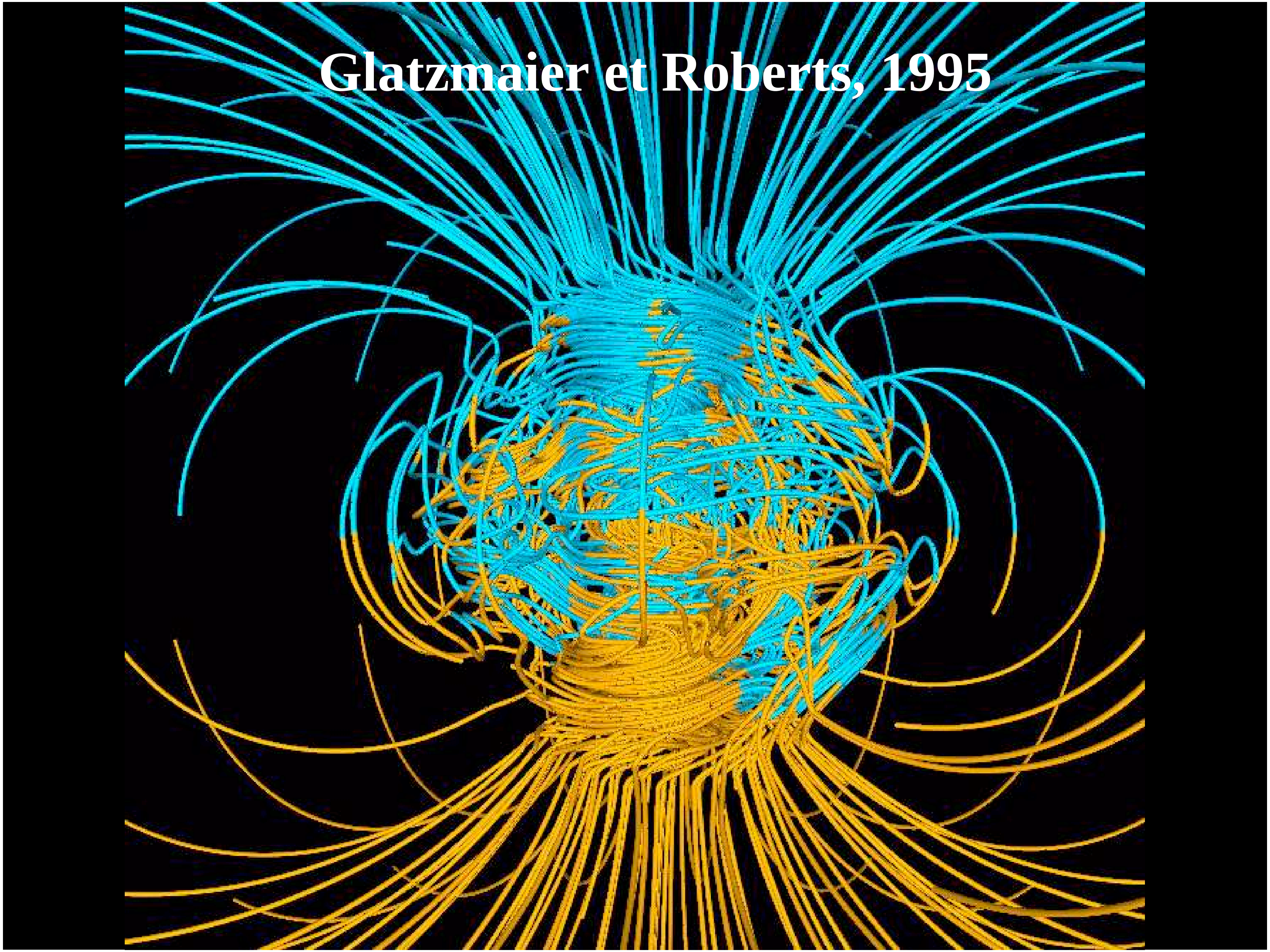
Glatzmaier et Roberts, 1995

Phys. Earth and Planet. Int., **91**, 63-75, 1995

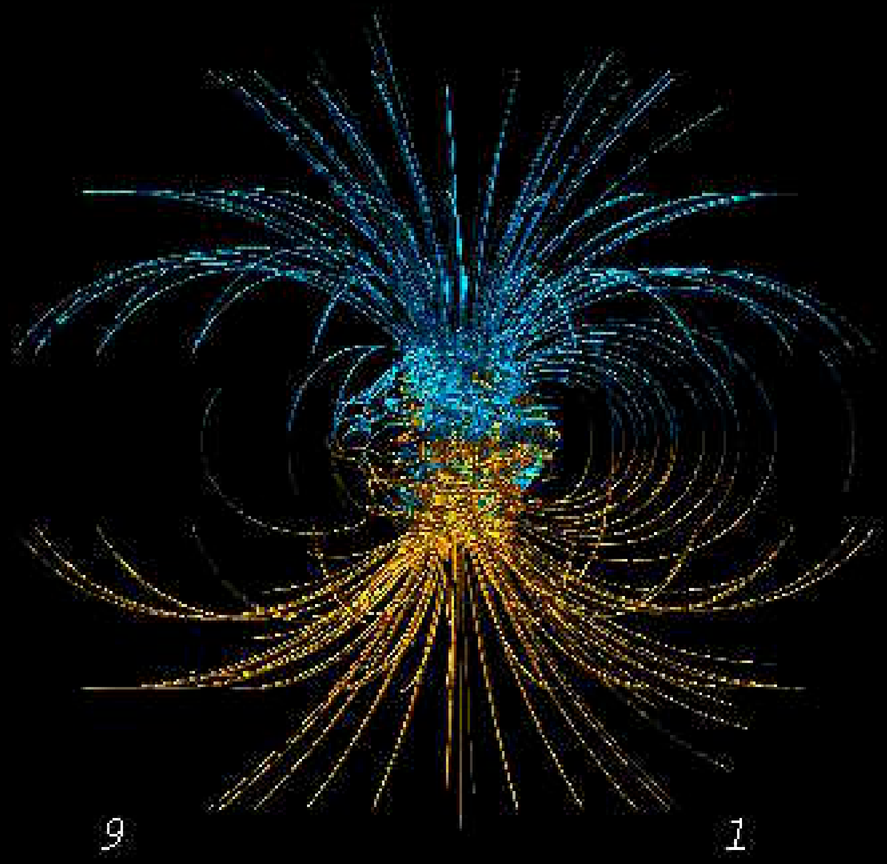

Nature, **377**, 203-209, 1995

[redacted]

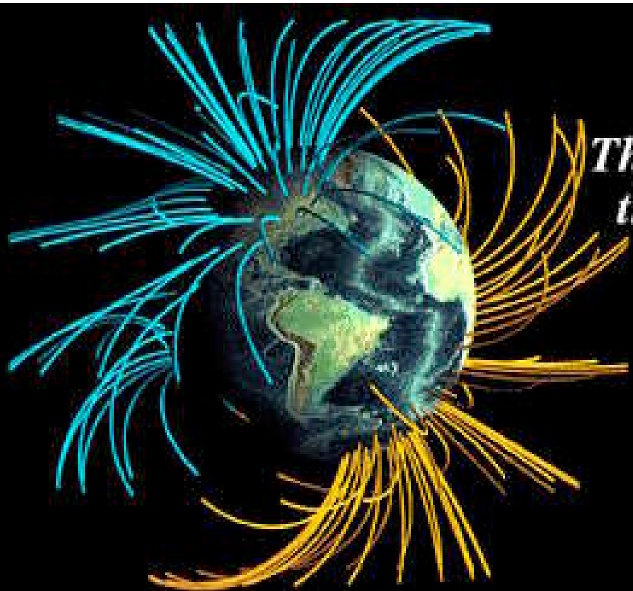

Their model offers the first coherent explanation of magnetic field reversal.

Kuang et Bloxham, 1997

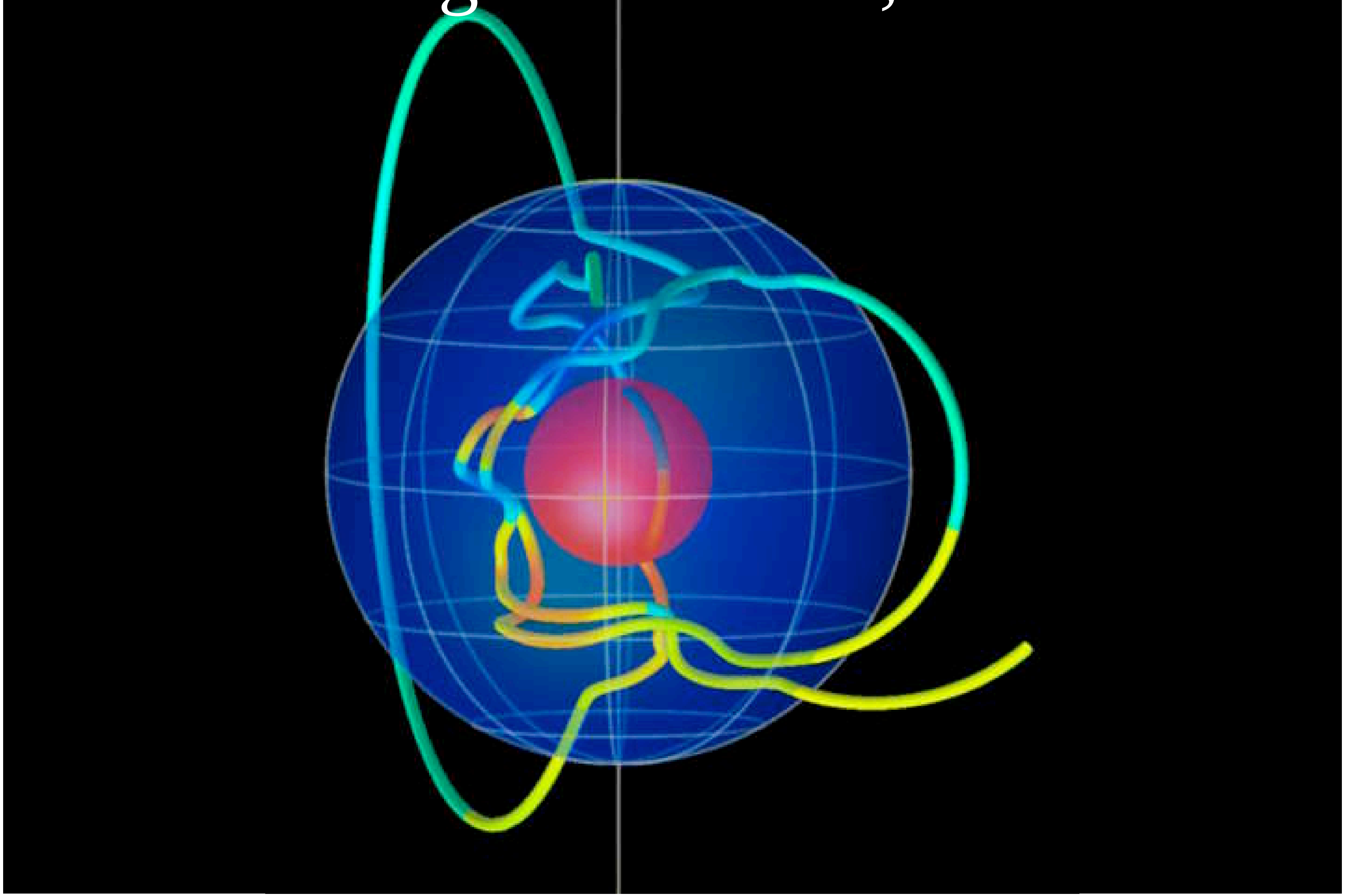

Kageyama et al., 1997

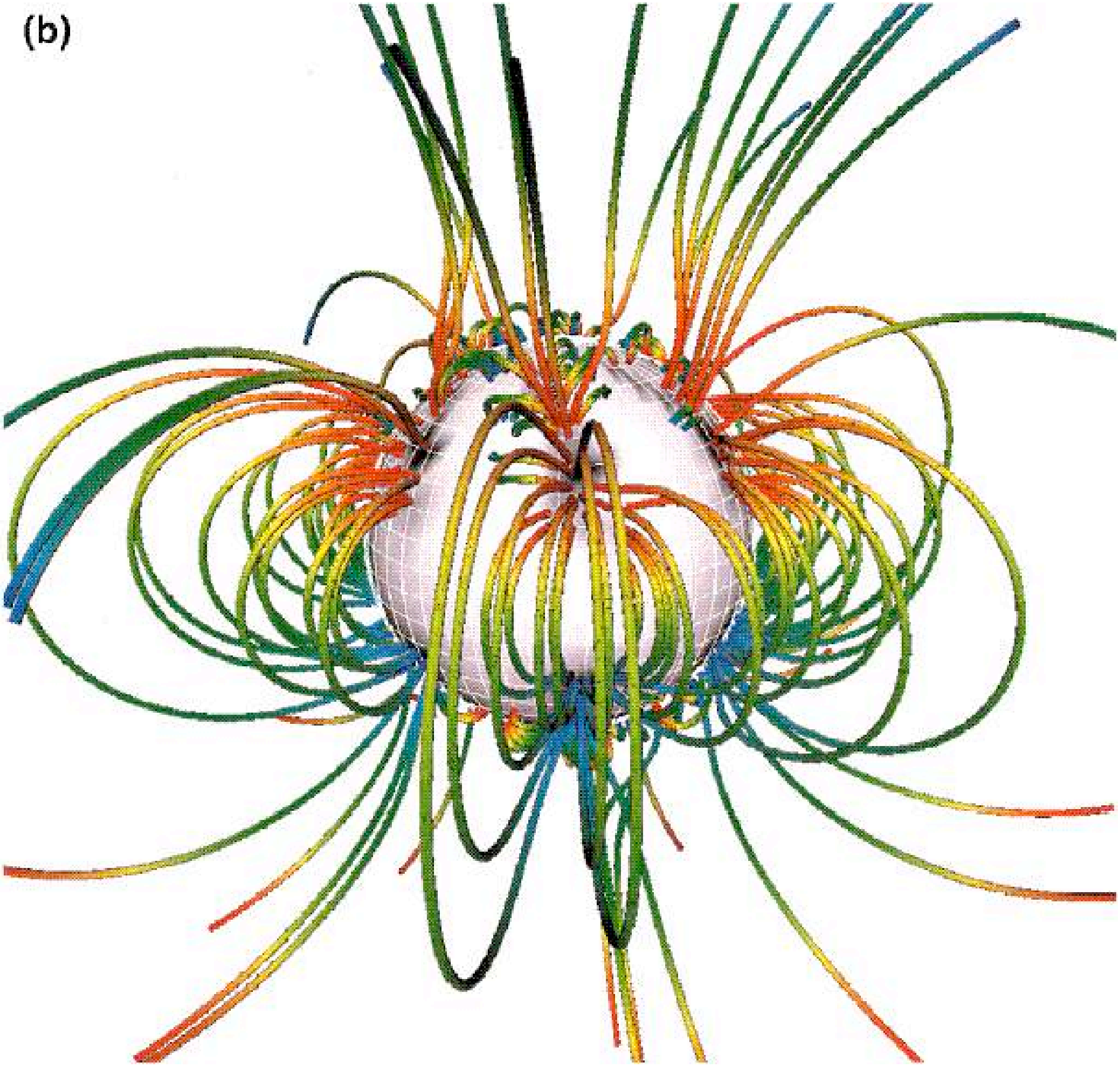

Christensen et al., 1998

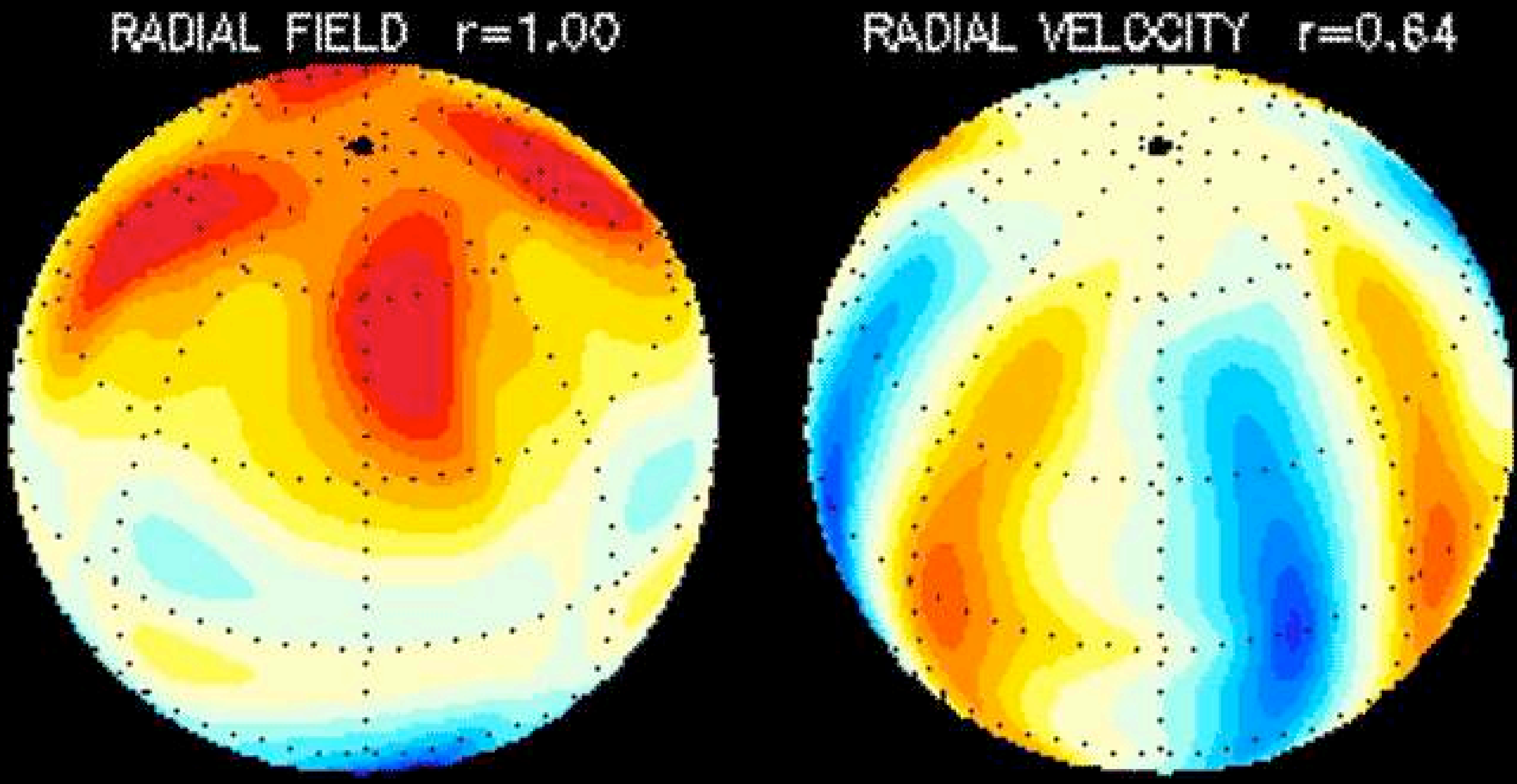

Results of the Dynamo Benchmark

Hiroaki Matsui

Radial velocity at mid-depth of the fluid

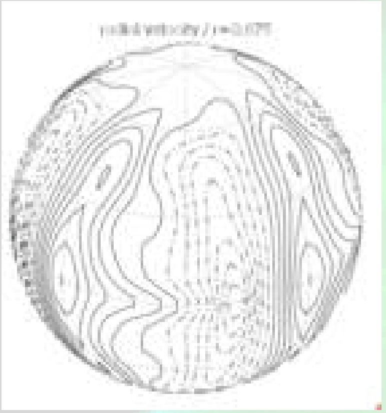

Christensen,2001

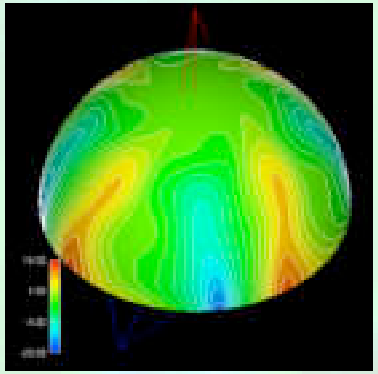

GeoFEM for t=12.0

Radial magnetic field at Core-Mantle boundary

Christensen,2001

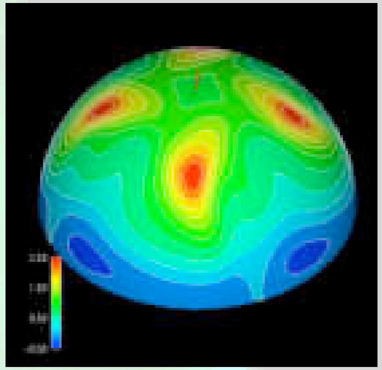

GeoFEM for t=12.0

Convergence of solutions

Averaged magnetic energy

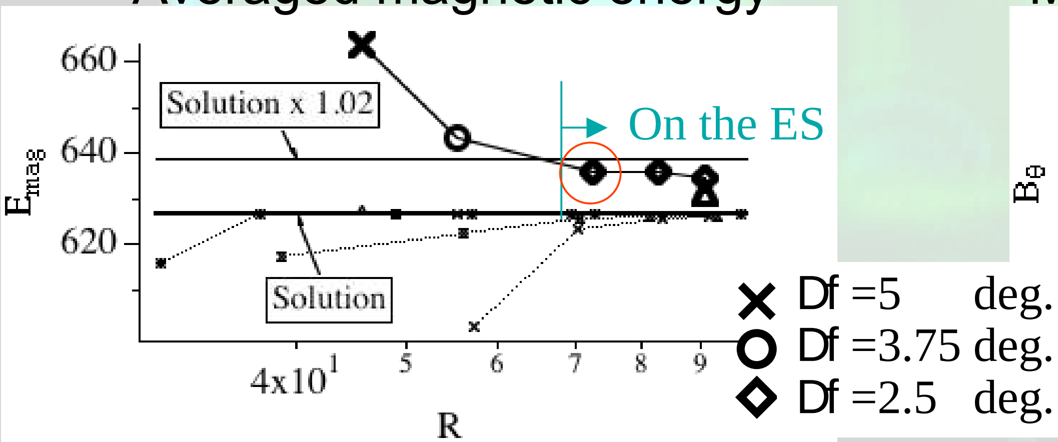

Magnetic field at a specific point

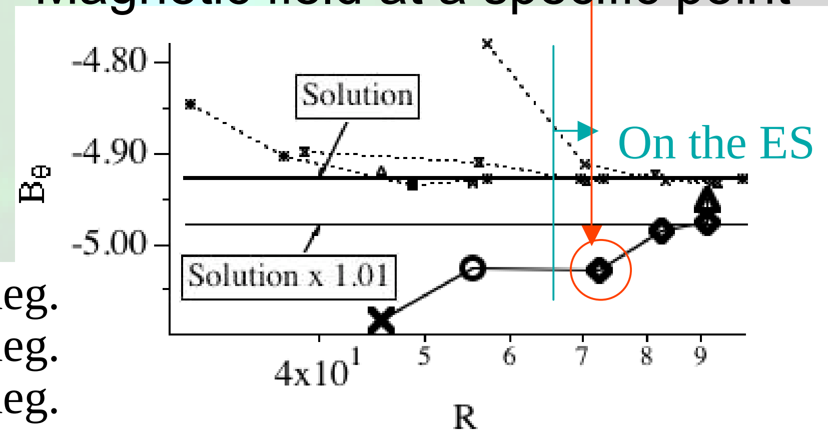

R is third root of DOF for scalar valuables

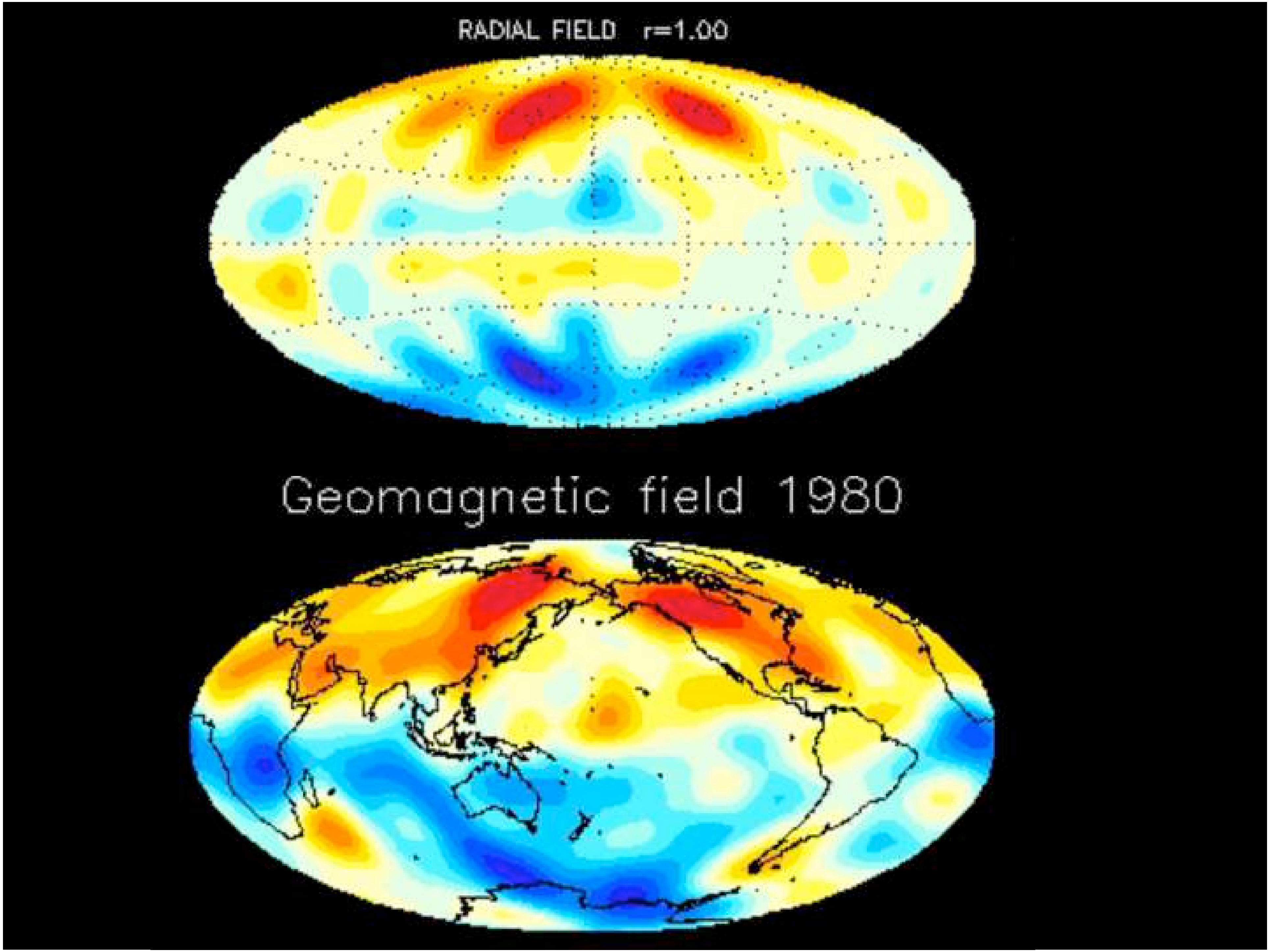
RADIAL FIELD r=1.00
Geomagnetic field 1980

Katayama et al., 1999

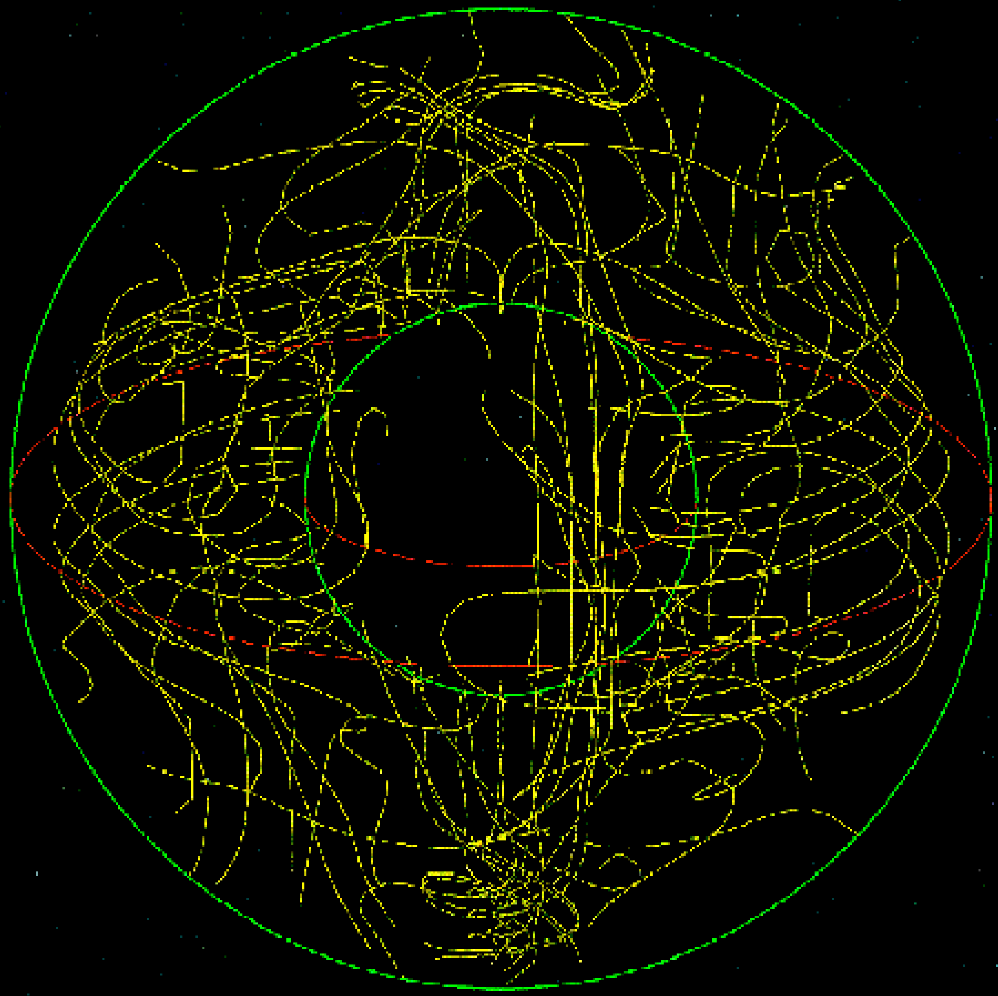

$$
\begin{cases}
Ro\left(\dfrac{\partial \mathbf{u}}{\partial t} + (\mathbf{u}\cdot\boldsymbol{\nabla})\,\mathbf{u}\right) + \mathbf{e}_z \wedge \mathbf{u} = -\boldsymbol{\nabla}\pi - q\,Ra\,E\,T\,\mathbf{g} + E\,\Delta\mathbf{u} \\
\qquad\qquad\qquad\qquad\qquad\qquad + (\boldsymbol{\nabla}\wedge\mathbf{B})\wedge\mathbf{B} \\
\boldsymbol{\nabla}\cdot\mathbf{u} = 0 \\
\dfrac{\partial T}{\partial t} + \mathbf{u}\cdot\boldsymbol{\nabla}T = q\Delta T \\
\dfrac{\partial \mathbf{B}}{\partial t} = \boldsymbol{\nabla}\wedge(\mathbf{u}\wedge\mathbf{B}) + \Delta\mathbf{B}
\end{cases}
$$

$$
Ro = \frac{\eta}{2\Omega\mathcal{L}^2} \qquad E = \frac{\nu}{2\Omega\mathcal{L}^2} \qquad q = \frac{\kappa}{\eta}
$$

	Parameters			Model		
	E $(\nu/\Omega r^2)$	*Pr* (ν/κ)	*Pm* (ν/η)	*Equations*	*Boundary Conditions*	*Integr. Time*
Glatzmaier-Roberts 1995	$\ell = 1$ $1.8 \cdot 10^{-6}$ $\ell = 10$ $1.3 \cdot 10^{-4}$ $\ell = 20$ $1.0 \cdot 10^{-3}$	5000	500	Boussinesq No-inertia	Conducting I.C., Ins. M. Rigid, with enhanced viscosity near boundaries	$3\tau_d$
Glatzmaier-Roberts 1996*a*	$\ell = 1$ $1.8 \cdot 10^{-6}$ $\ell = 10$ $1.3 \cdot 10^{-4}$ $\ell = 20$ $1.0 \cdot 10^{-3}$	5000	500	Boussinesq Axial-inertia	Conducting I.C. Ins. mantle Rigid	$0.8\tau_d$
Glatzmaier-Roberts 1996*b* and following	$\ell = 1$ $1.8 \cdot 10^{-6}$ $\ell = 10$ $6.5 \cdot 10^{-5}$ $\ell = 20$ $5.1 \cdot 10^{-4}$	725	725	Anelastic Axial-inertia	Conducting I.C. Ins. mantle Rigid	$15\tau_d$
Kuang-Bloxham	$\ell = 1$ $4.0 \cdot 10^{-5}$ $\ell = 10$ $9.0 \cdot 10^{-5}$ $\ell = 20$ $4.9 \cdot 10^{-4}$	1	1	Boussinesq Axial-inertia	Conducting I.C. Ins.M.+conducting layer Stress-free	$2\tau_d$
Busse et al.	$5.1 \cdot 10^{-4}$–$7.2 \cdot 10^{-4}$	5–20	100	Boussinesq Full-inertia	Ins. M. & I.C. Stress-free	$1.4\tau_d$
Kageyama et al.	$4.0 \cdot 10^{-4}$	1	10.6–15	Compressible Full-inertia	$B \wedge r = 0$ Rigid	$50\tau_d$
Christensen et al.	$4.2 \cdot 10^{-5}$–$4.2 \cdot 10^{-4}$	1	0.5–5	Boussinesq Full-inertia	Ins. M. & I.C. Rigid or Stress-free	$3\tau_d$ to $10\tau_d$
Kitauchi-Kida	$5.6 \cdot 10^{-3}$	1	8.3–14.2	Boussinesq Full inertia	Vacuum Rigid	$100\tau_d$
Sakuraba-Kono	$\ell = 1$ $6.3 \cdot 10^{-5}$ $\ell = 10$ $7.1 \cdot 10^{-5}$ $\ell = 20$ $1.3 \cdot 10^{-4}$	1	20	Boussinesq Full inertia	Conducting I.C. Ins. mantle Rigid	$3\tau_d$
Katayama et al.	$7.2 \cdot 10^{-3}$–$7.2 \cdot 10^{-2}$	1	35	Boussinesq Full inertia	Ins. M. & I.C. Stress-free	$6\tau_d$
Earth	10^{-15}	1/7	10^{-6}			

	Outputs				
	Dipolar Field	Λ (F_B/F_Ω)	*Reversals*	*Westward Drift*	*Others*
Glatzmaier-Roberts 1995	*Yes*	500	*Yes*	*Yes*	Spectrum I.C. Super-rot.
Glatzmaier-Roberts 1996*a*	*Yes*		Not yet	*Yes*	Spectrum I.C. Super-rot.
Glatzmaier-Roberts 1996*b* and following	*Yes*	100	*Yes*	*Yes*	Spectrum I.C. Super-rot.
Kuang-Bloxham	*Yes*	$\mathcal{O}(1)$	Not yet	*Yes*	Flux Expulsion Pacific window Spectrum
Busse et al.	*Yes*	2–20	Not yet		
Kageyama et al.	*Yes*	$7 \cdot 10^{-4}$	*Yes*		Patches Sawtooth?
Christensen et al.	*Yes*	0.14–14	Not yet	*Yes*	Patches
Kitauchi-Kida	*Yes*	60	*Yes*	*Yes*	Quasi 3 fold symmetry
Sakuraba-Kono	*Yes*	0.1–10	Not yet		Archean paleointensity
Katayama et al.	*Yes*	$6 \cdot 10^{-4}$	Not yet	*Yes*	
Earth		$\mathcal{O}(1)$?			

Sawtooth, SINT800

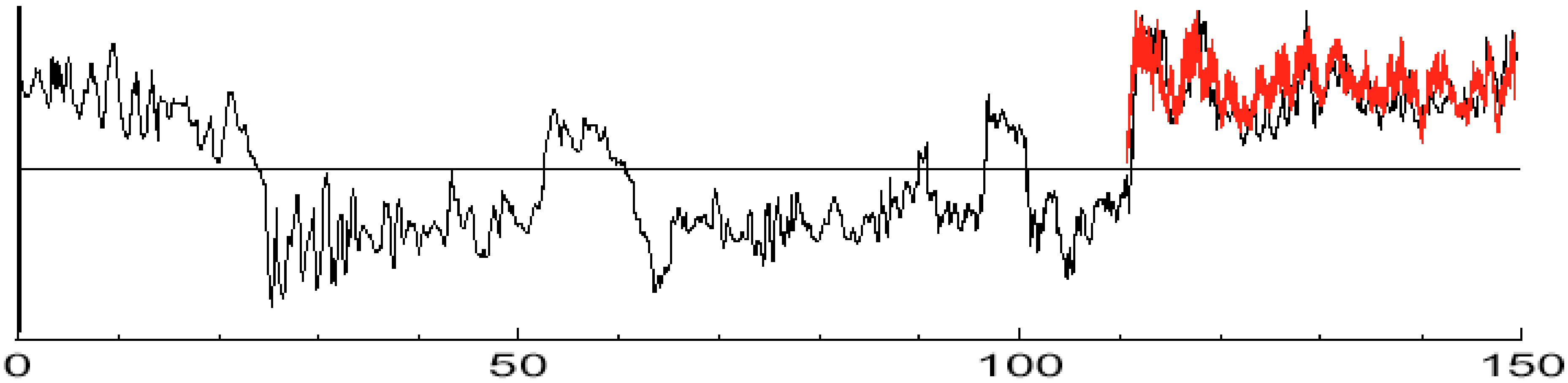

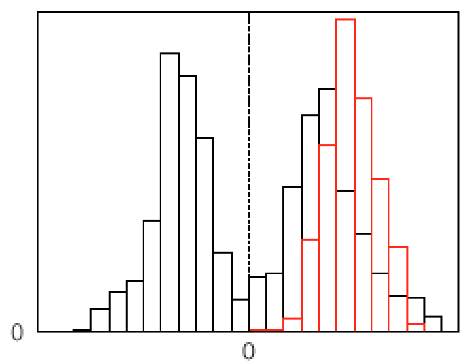

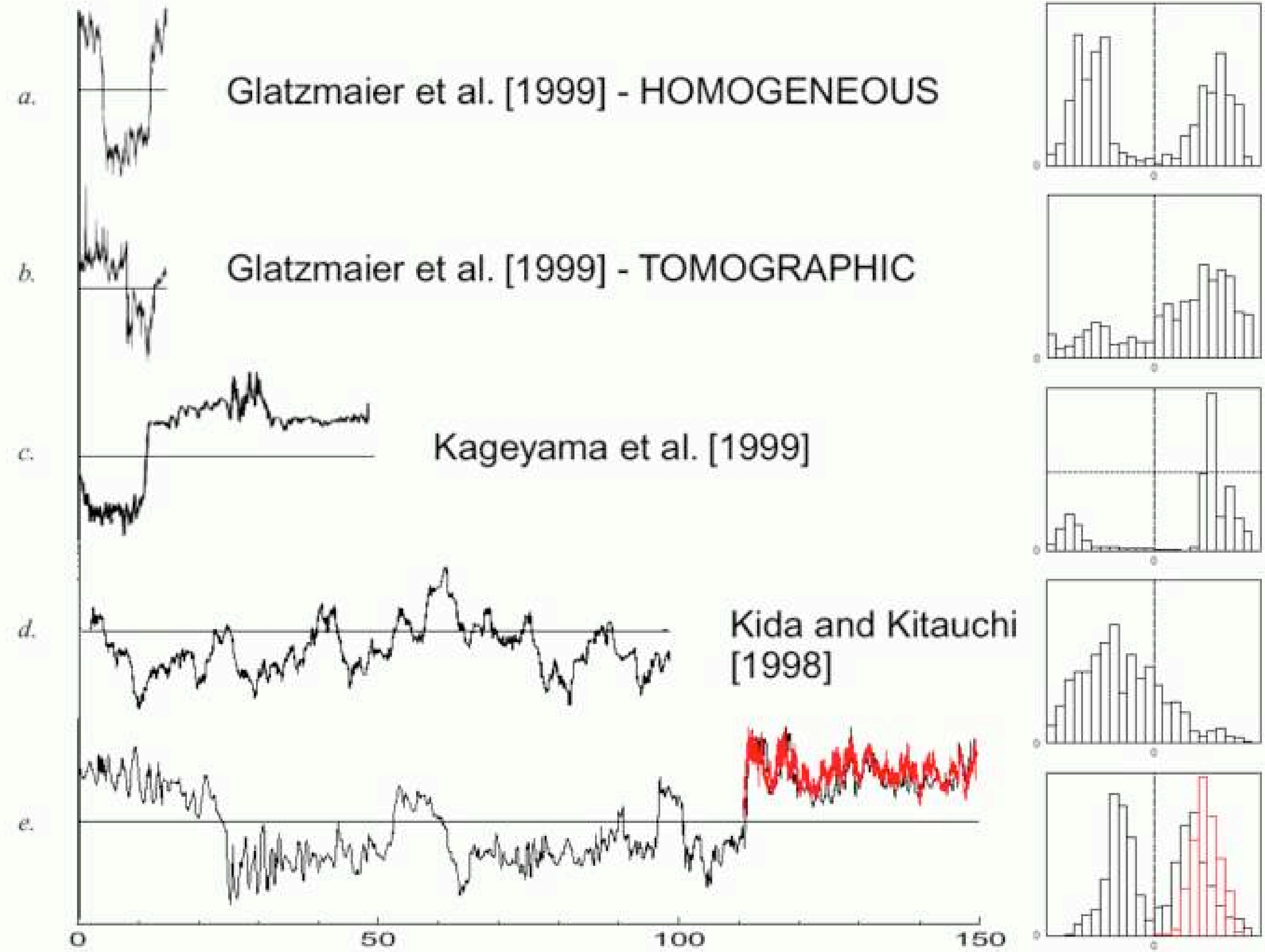

a.
Glatzmaier et al. [1999] - HOMOGENEOUS
b.
Glatzmaier et al. [1999] - TOMOGRAPHIC
c.
Kageyama et al. [1999]
d.
Kida and Kitauchi [1998]
e.
0
50
100
150

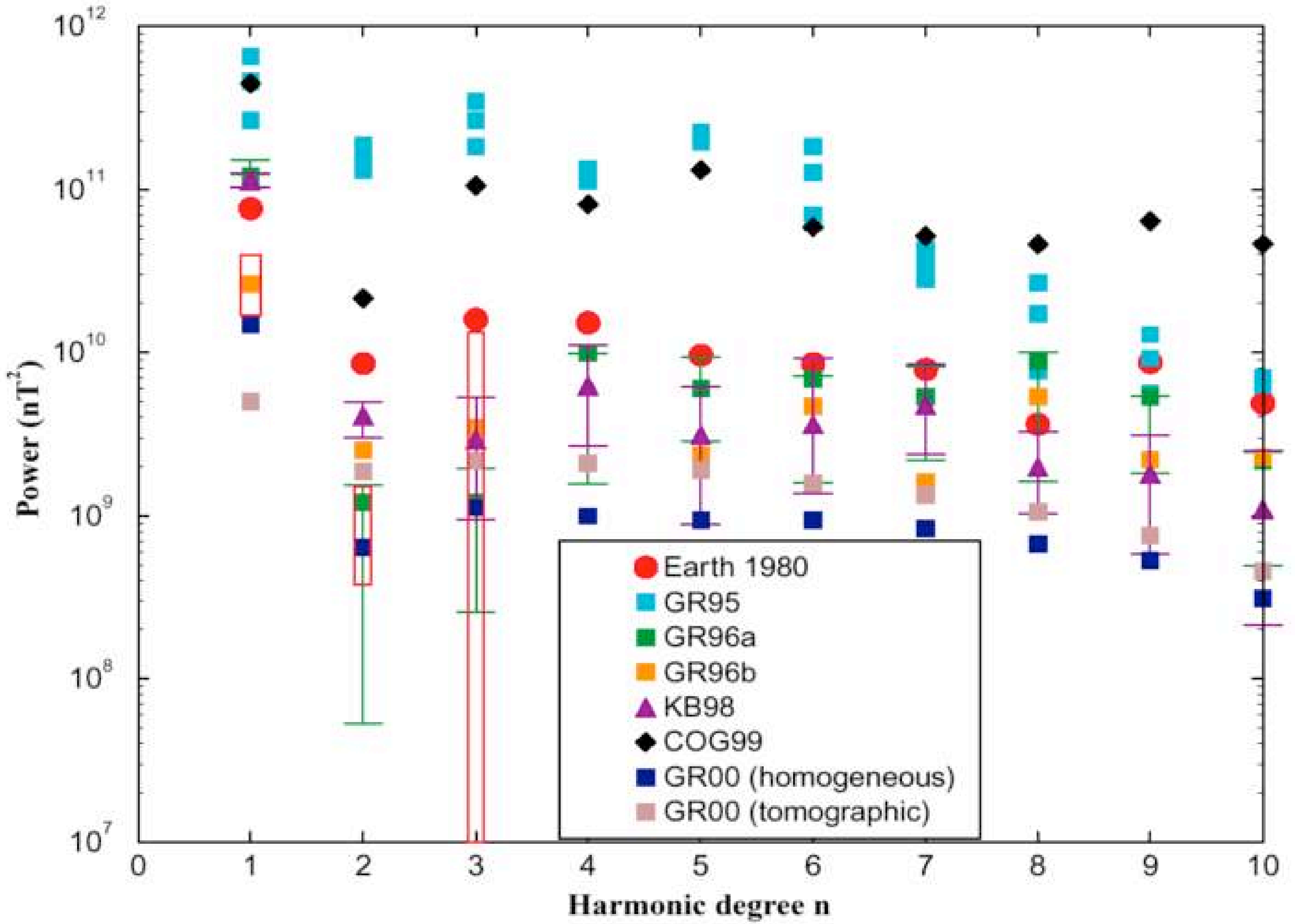

Dormy et al.,G-cubed, **1**, 62, 2000

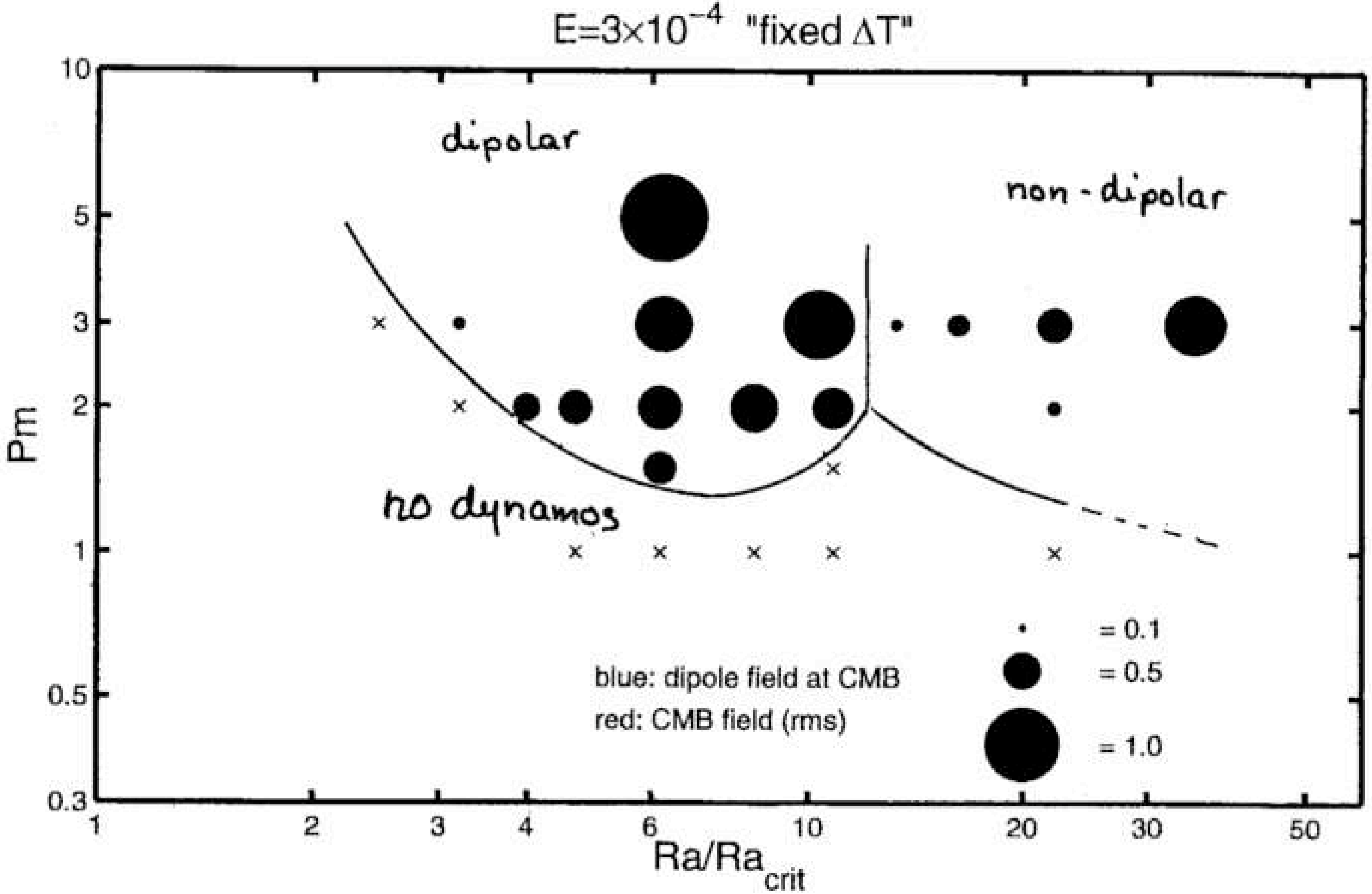

Christensen et al. 2003

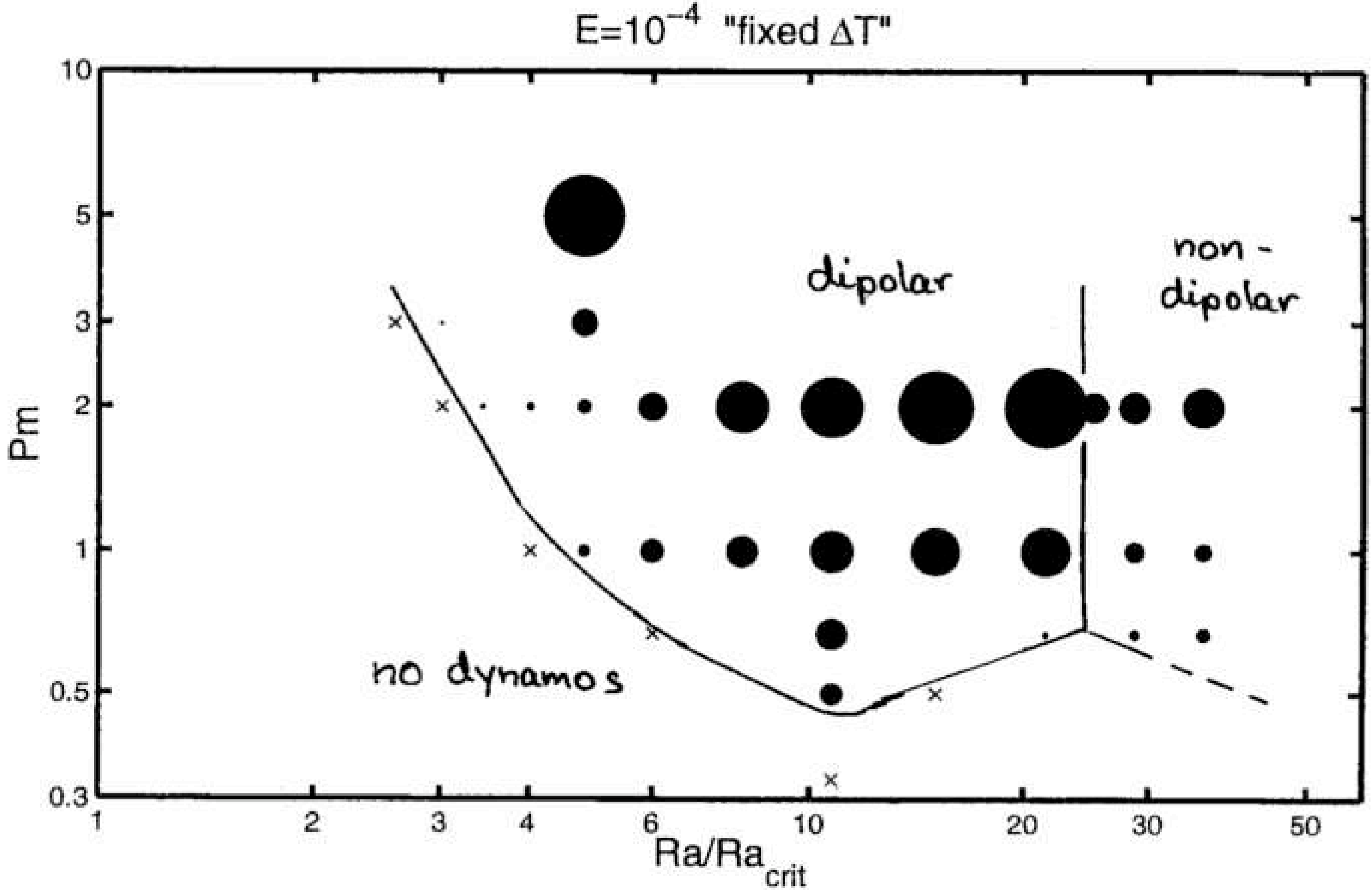

Christensen et al. 2003

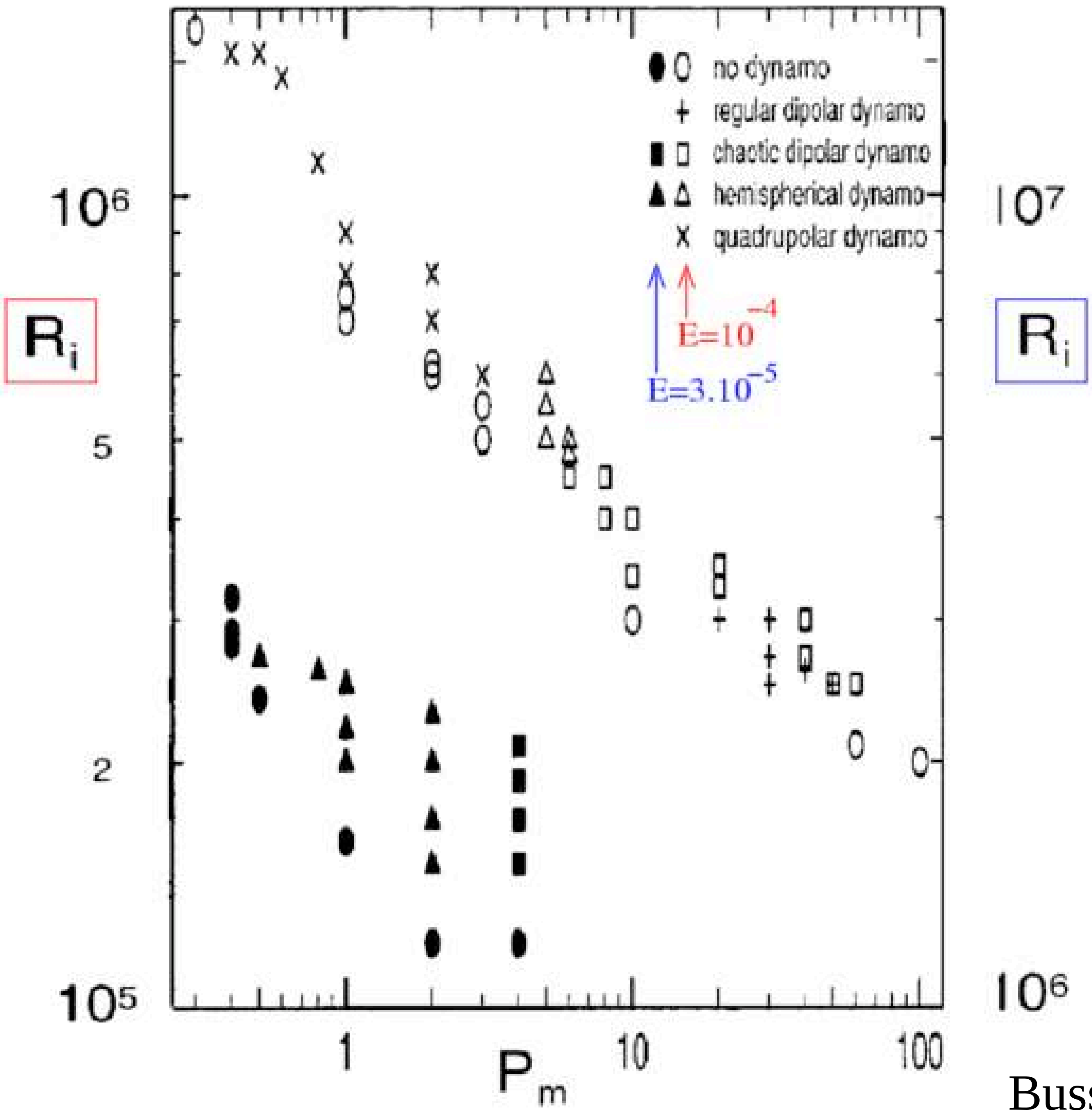
10⁶
5
2
10⁵
Rᵢ
10⁷
10⁶
Rᵢ
no dynamo
regular dipolar dynamo
chaotic dipolar dynamo
hemispherical dynamo
quadrupolar dynamo
E=10⁻⁴
E=3.10⁻⁵
1
10
100
Pₘ

Busse, 2002